Fluorescence fiber-optic turn-on detection of trace hydrazine vapor with dicyanovinyl-functionalized triazatruxene-based hyperbranched conjugated polymer nanoparticles

Yuxiang Xu[a,b], Hua Li[a,b], Xiaofu Wu[a], Yonghong Chen[a,c], Hao Hang[a,b], Hui Tong[a]*, Lixiang Wang[a]*

[a]*State Key Laboratory of Polymer Physics and Chemistry, Changchun Institute of Applied Chemistry, Chinese Academy of Sciences, Changchun 130022, P. R. China.*

[b]*University of Chinese Academy of Sciences, Beijing 100049, P. R. China.*

[c]*University of Science and Technology of China, Hefei 230026, P. R. China.*

Supporting Information

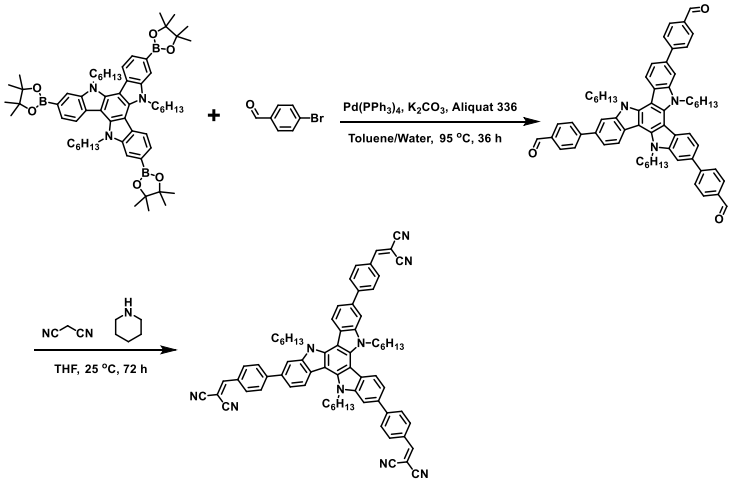

Scheme S1. Synthesis of **TAT-DCV**.

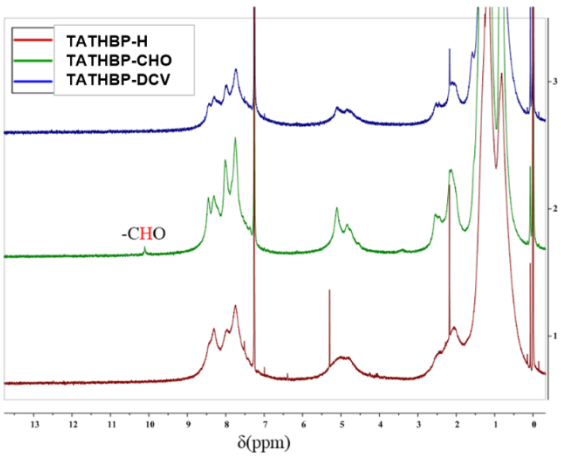

Fig. S1 ^{1}H NMR spectra of **TATHBP-H**, **TATHBP-CHO** and **TATHBP-DCV** in $CDCl_3$.

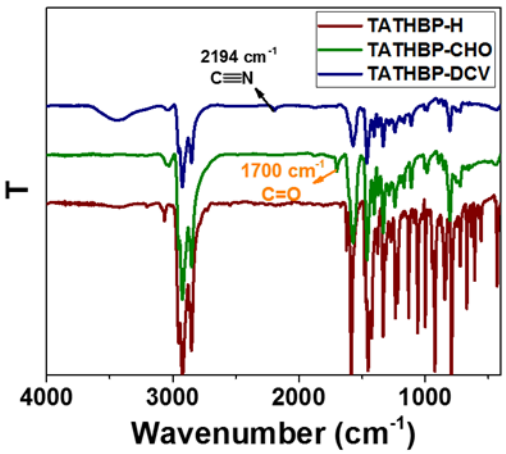

Fig. S2 FT-IR spectra of **TATHBP-H**, **TATHBP-CHO** and **TATHBP-DCV**.

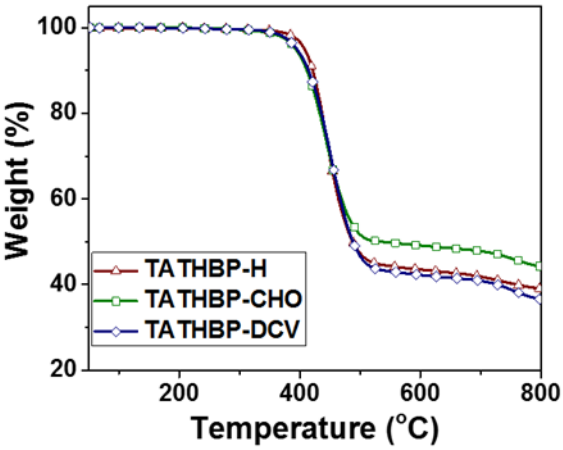

Fig. S3 TGA curves of **TATHBP-H**, **TATHBP-CHO** and **TATHBP-DCV** recorded under N_2 atmosphere.

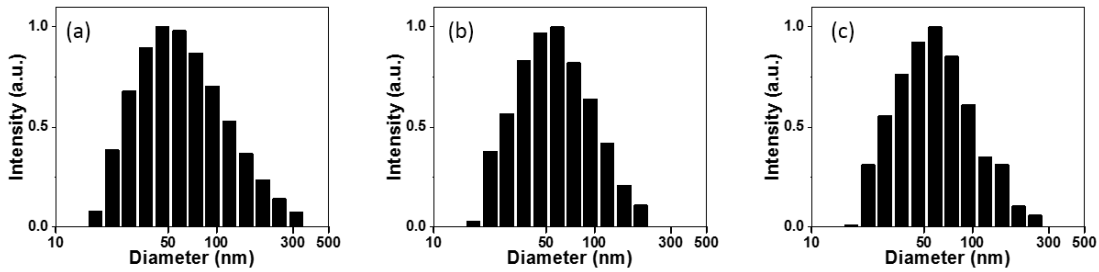

Fig. S4 Hydrodynamic diameters of **TATHBP-H** (a), **TATHBP-CHO** (b), and **TATHBP-DCV** (c) measured by dynamic light scattering.

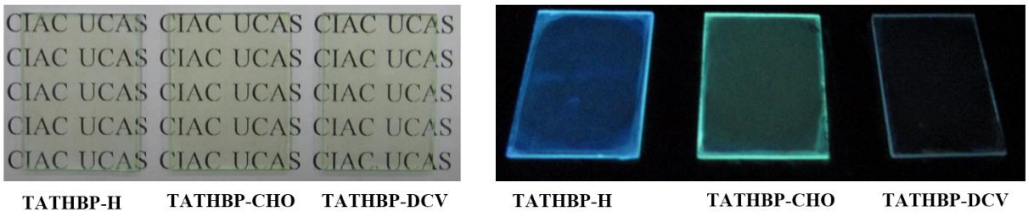

Fig. S5 Images of **TATHBP-H**, **TATHBP-CHO** and **TATHBP-DCV** films coated on glass substrates under sunlight (left) and UV light(right).

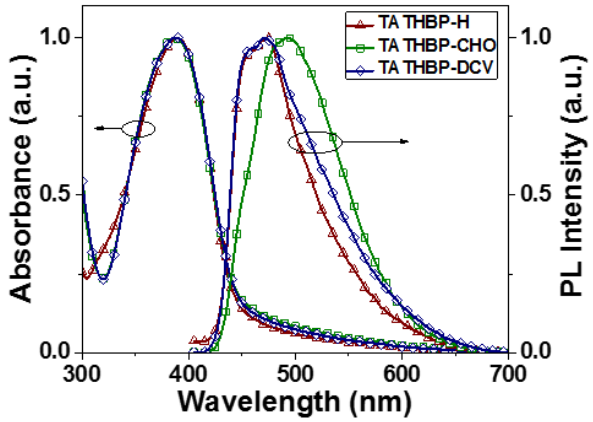

Fig. S6 UV-vis absorption and PL spectra of **TATHBP-H**, **TATHBP-CHO** and T**ATHBP-DCV** spin-coated films.

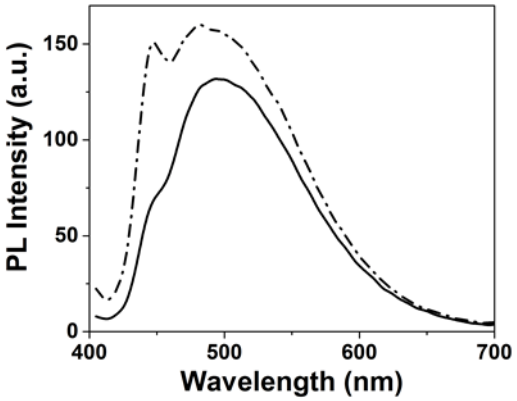

Fig. S7 PL spectra of spin-coated film of **TATHBP-CHO** on glass substrates before (solid) and after exposure to saturated hydrazine vapor for 12 hour (dash-dot).

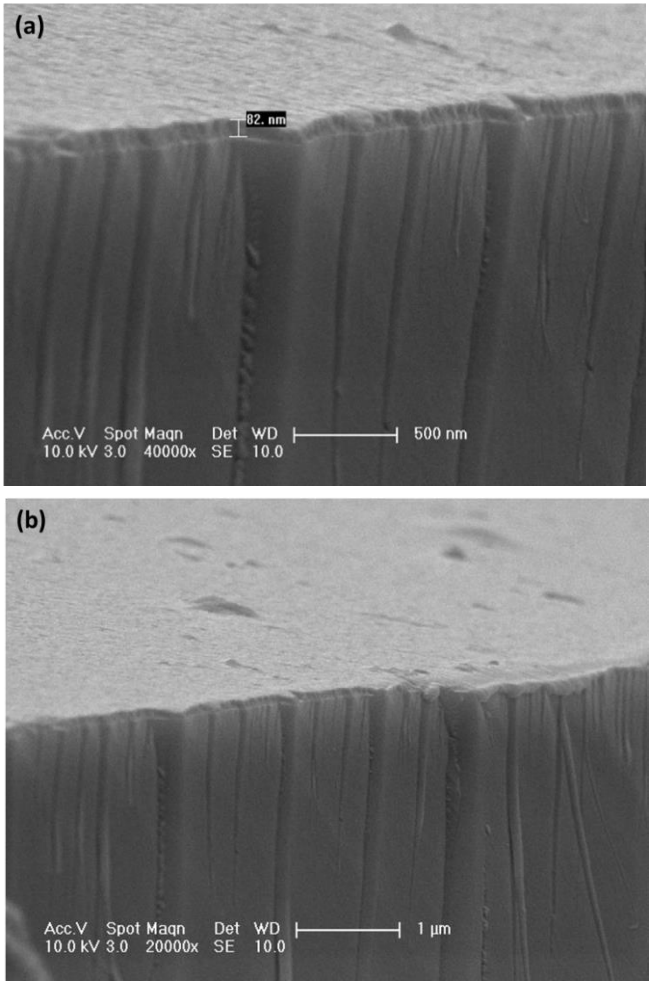

Fig. S8 Two SEM images of the **TATHBP-DCV** film coated on fiber-optic tip.

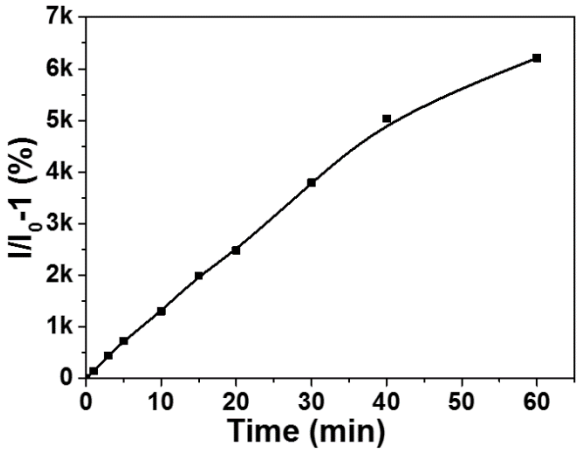

Fig. S9 Time-dependent fluorescence enhancement of **TATHBP-DCV** film coated on fiber-optic tip upon exposure to hydrazine vapor.

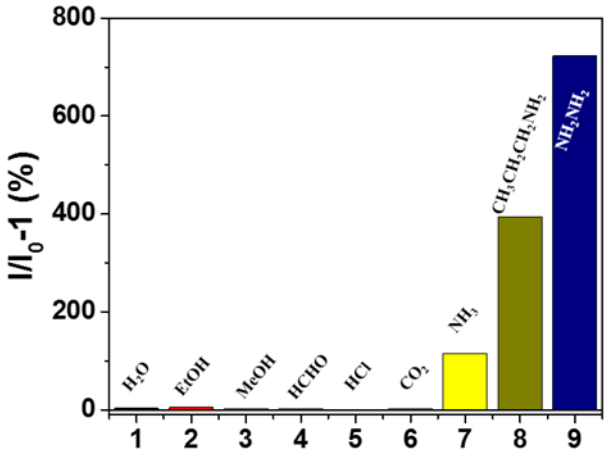

Fig. S10 Fluorescent enhancement of **TATHBP-DCV** coated fiber-optic tips upon exposure to hydrazine and other common interference vapors for 5 min.

Table S1 A list of recently reported fluorescence sensors for detection of hydrazine vapor.

Publication	Probe's chemical structure	Limit of Detection	Detection method
This work	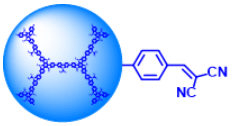	1.1 mg/m^3 0.01% solution (aq.)	Optic-fiber for 5 min based on fluorescence turn on detection
Adv. Mater. **2006**, 18, 1047-1050	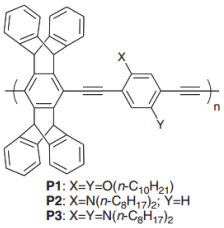 P1: X=Y=O(*n*-$C_{10}H_{21}$) P2: X=N(*n*-C_8H_{17})$_2$, Y=H P3: X=Y=N(*n*-C_8H_{17})$_2$	100 ppb	Fido sensing platform based on fluorescence enhancement
Chem. Sci., **2013**, 4, 4121–4126	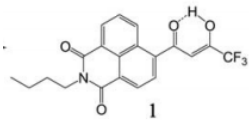 1	n.d.	TLC plates for 1.0 min based on fluorescence turn on detection at hydrazine vapor (9.0 mmHg)
*RSC Adv.***2013**, 3, 17924-17929	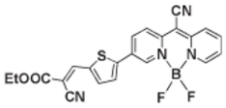 PBF_2	n.d.	silica plates for a few minutes based on ratiometric fluorescence detection at hydrazine vapor (14.4 mmHg)
*Anal. Chem.***2014**, 86, 4611−461	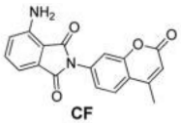 CF	5.4 mg/m^3 0.05% solution (aq.)	TLC plates for 10 min based on ratiometric fluorescence detection
Anal. Methods, **2014**,6, 4705-4709	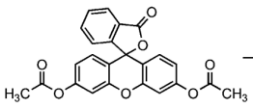	0.4% solution (aq.)	Nylon 66 microporous membranes for 10 min based on fluorescence "switch-on" approach
*Anal. Chem.***2015**, 87, 9101-9107	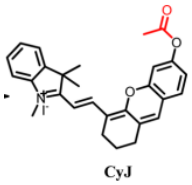 CyJ	0.1% solution (aq.)	filter papers for 15 min based on Near-Infrared fluorescence turn on detection
Chem. Commun., **2014**,50, 1485-1487	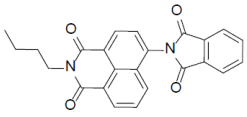	111.7 mg m^{-3} 1% solution (aq.)	TLC plates for 10 min based on fluorescence turn on detection at hydrazine vapor

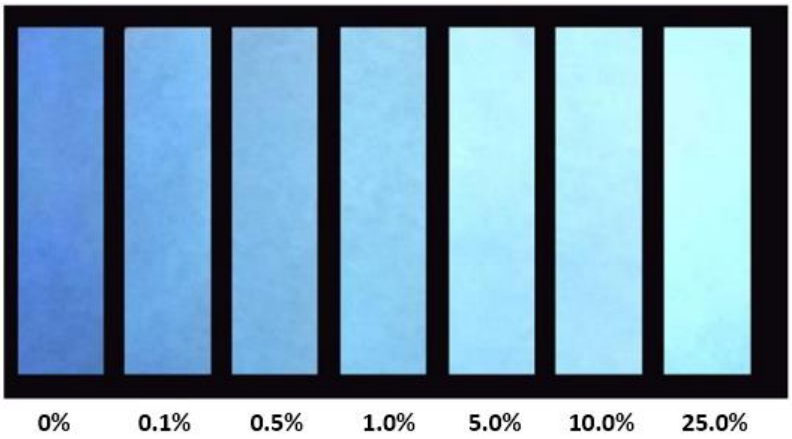

Fig. S11 Fluorescent images of **TATHBP-DCV**-coated filter papers after exposure to hydrazine vapor from aqueous hydrazine solutions with different hydrazine concentrations.

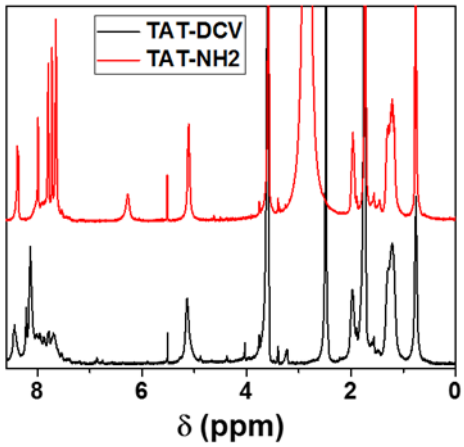

Fig. S12 ^{1}H NMR spectra of **TAT-DCV** and **TAT-NH2** in THF-d_8.

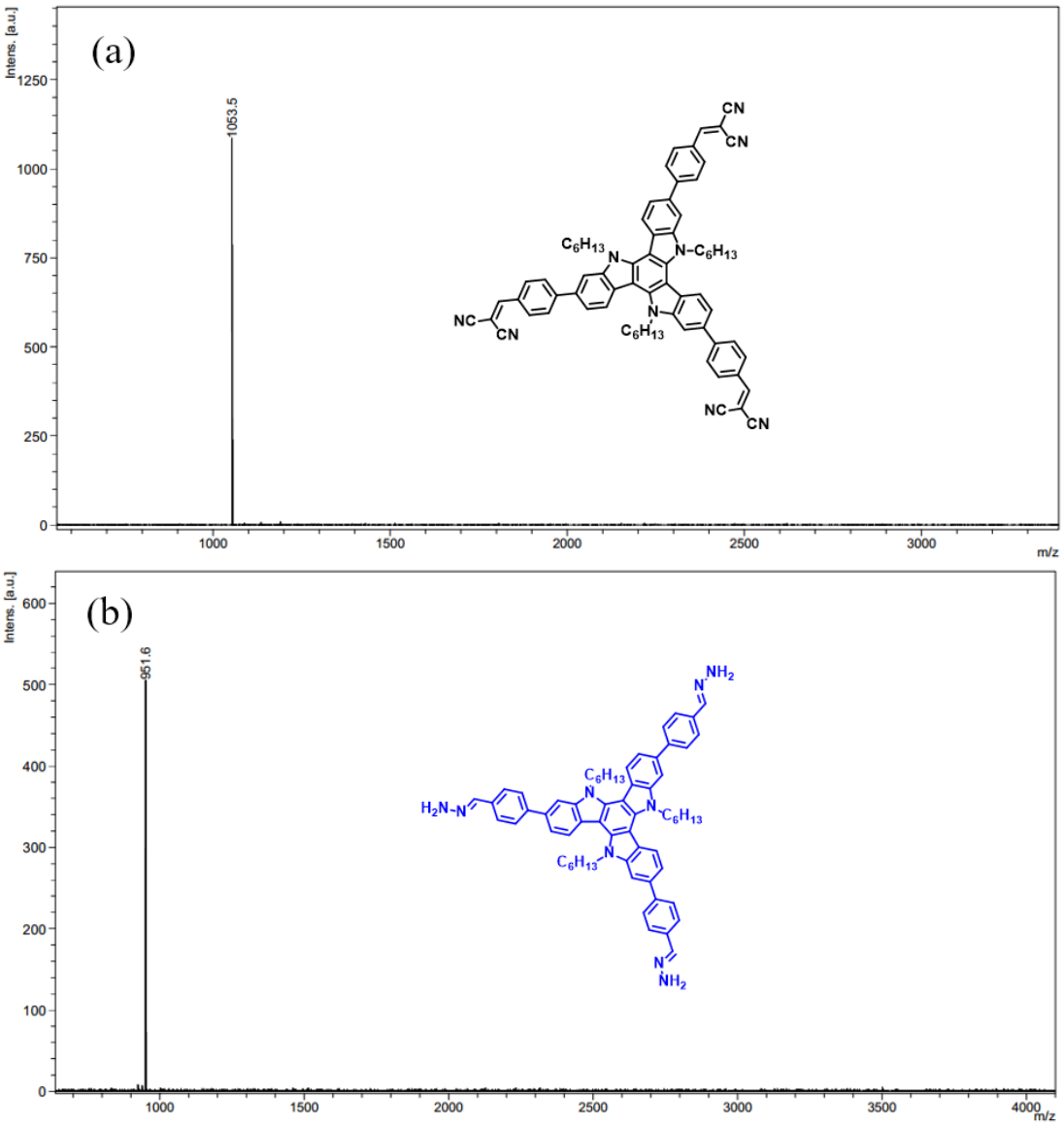

Fig. S13 MALDI-TOF MS spectra of **TAT-DCV** (a) **and TAT-NH2** (b).

MALDI-TOF MS (m/z) of **TAT-DCV**: Calcd. for $C_{72}H_{63}N_9$, $[M]^+$: 1053.5; Found: 1053.5.
MALDI-TOF MS (m/z) of **TAT-NH2**: Calcd. for $C_{63}H_{69}N_9$, $[M]^+$: 951.6; Found: 951.6.

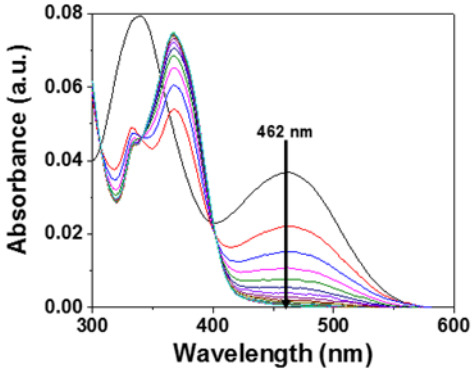

Fig. S14 Absorption spectral changes of **TAT-DCV** solution after addition of hydrazine hydrate.

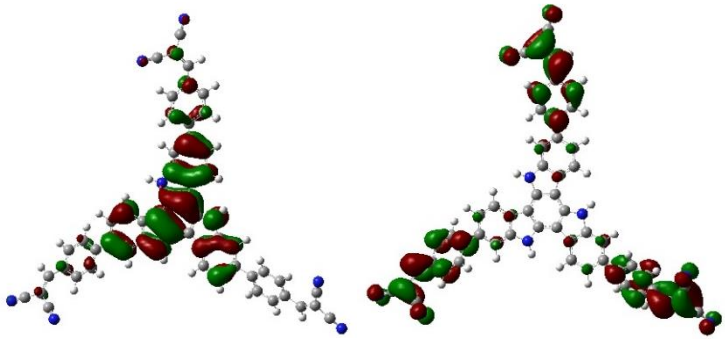

HOMO LUMO

Fig. S15 HOMO and LUMO of **TAT-DCV** calculated at the B3LYP/6-31G (d) level.

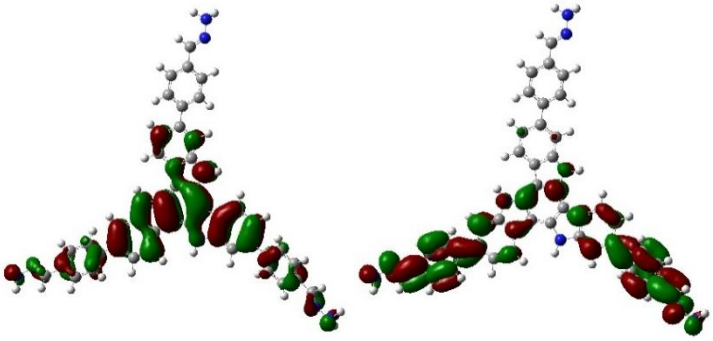

HOMO LUMO

Fig. S16 HOMO and LUMO of **TAT-NH2** calculated at the B3LYP/6-31G (d) level.

Molecular geometries of two model compounds for **TAT-DCV** and **TAT-NH2** were optimized using density functional theory at the B3LYP/6-31G(d) level. To simplify the calculation, the alkyl groups on the triazatruxene units are replaced by hydrogen atoms. Frequency calculations were performed at the B3LYP/6-31G(d) level. The isodensity coefficient used to illustrate the HOMO/LUMO is 0.02. All calculations were carried out using the Gaussian 03 suite of programs.

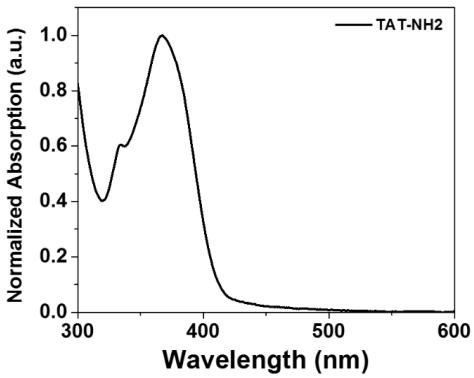

Fig. S17 UV-Vis Absorption spectrum of **TAT-NH2** in THF.

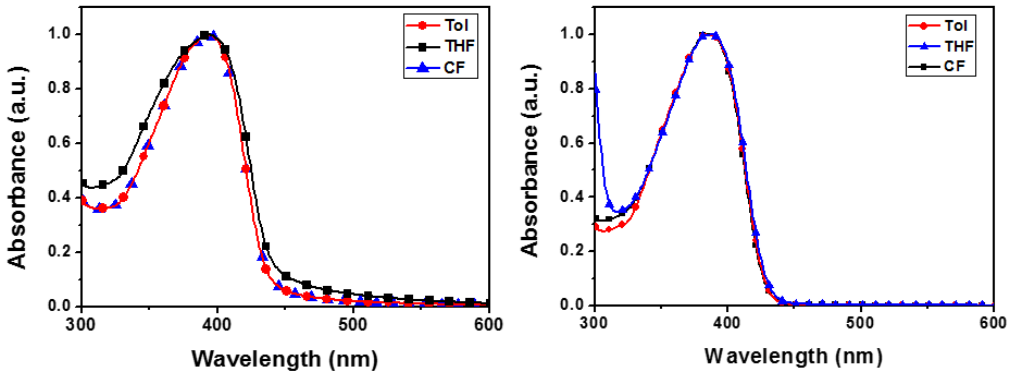

Fig. S18 Absorption spectra of **TATHBP-CHO** (a) and **TATHBP-DCV** (b) in varying solvents.

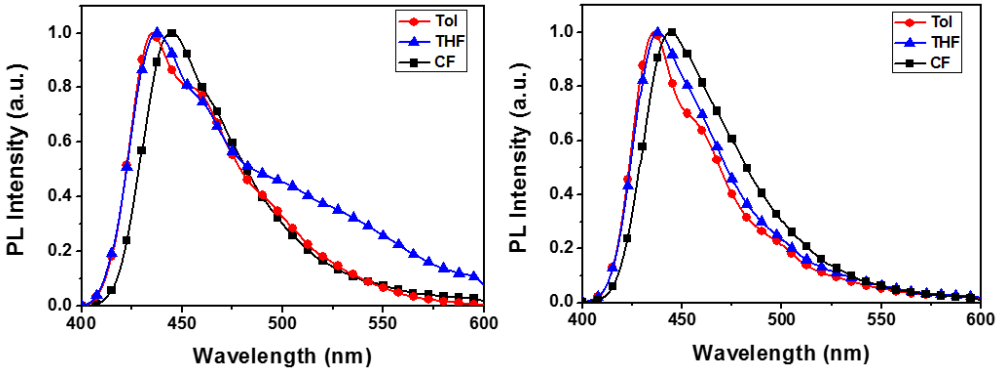

Fig. S19 Emission spectra of **TATHBP-CHO** (a) and **TATHBP-DCV** (b) in varying solvents.